Hydrodynamic Diffusion and Its Breakdown near AdS_2 Quantum Critical Points

Citation for published version:
Areán, D, Davison, RA, Goutéraux, B & Suzuki, K 2021, 'Hydrodynamic Diffusion and Its Breakdown near AdS_2 Quantum Critical Points', *Physical Review X*, vol. 11, no. 3, 031024. https://doi.org/10.1103/PhysRevX.11.031024

Digital Object Identifier (DOI):
10.1103/PhysRevX.11.031024

Published In:
Physical Review X

Hydrodynamic Diffusion and Its Breakdown near AdS_2 Quantum Critical Points

Daniel Areán[*]
Instituto de Física Teórica UAM/CSIC and Departamento de Física Teórica, Universidad Autónoma de Madrid Campus de Cantoblanco, 28049 Madrid, Spain

Richard A. Davison[†]
Department of Mathematics and Maxwell Institute for Mathematical Sciences, Heriot-Watt University, Edinburgh EH14 4AS, United Kingdom

Blaise Goutéraux[‡] and Kenta Suzuki[§]
CPHT, CNRS, Ecole polytechnique, IP Paris, F-91128 Palaiseau, France

(Received 12 February 2021; revised 22 April 2021; accepted 25 May 2021; published 29 July 2021)

Hydrodynamics provides a universal description of interacting quantum field theories at sufficiently long times and wavelengths, but breaks down at scales dependent on microscopic details of the theory. In the vicinity of a quantum critical point, it is expected that some aspects of the dynamics are universal and dictated by properties of the critical point. We use gauge-gravity duality to investigate the breakdown of diffusive hydrodynamics in two low-temperature states dual to black holes with AdS_2 horizons, which exhibit quantum critical dynamics with an emergent scaling symmetry in time. We find that the breakdown is characterized by a collision between the diffusive pole of the retarded Green's function with a pole associated to the AdS_2 region of the geometry, such that the local equilibration time is set by infrared properties of the theory. The absolute values of the frequency and wave vector at the collision (ω_{eq} and k_{eq}) provide a natural characterization of all the low-temperature diffusivities D of the states via $D = \omega_{\mathrm{eq}}/k_{\mathrm{eq}}^2$, where $\omega_{\mathrm{eq}} = 2\pi\Delta T$ is set by the temperature T and the scaling dimension Δ of an operator of the infrared quantum critical theory. We confirm that these relations are also satisfied in a Sachdev-Ye-Kitaev chain model in the limit of strong interactions. Our work paves the way toward a deeper understanding of transport in quantum critical phases.

DOI: 10.1103/PhysRevX.11.031024

Subject Areas: Condensed Matter Physics, Particles and Fields, String Theory

I. INTRODUCTION

Interacting quantum field theories are notoriously challenging, especially when there is no quasiparticle-based description of the state. To describe the late time, long wavelength dynamics of these states, one can instead rely on effective approaches such as hydrodynamics. This approach has been used to gain insight into the quark-gluon plasma [1–4], ultracold atomic systems [5], and electronic transport in metals [6–12].

[*]daniel.arean@uam.es
[†]r.davison@hw.ac.uk
[‡]blaise.gouteraux@polytechnique.edu
[§]kenta.suzuki@polytechnique.edu

At long times and wavelengths, hydrodynamics provides an effective description of a system in terms of a few conserved quantities dictated by symmetries [13–15]. Their evolution is governed by local conservation equations for the densities and associated currents, along with constitutive relations expressing the currents in terms of the densities in a gradient expansion. The late time relaxation of the system back to equilibrium is governed by the hydrodynamic modes: poles of the retarded Green's functions of the densities with gapless dispersion relations [16].

While extremely powerful, hydrodynamics breaks down at sufficiently short scales set by the local equilibration time and length. At such scales, the dynamics of the system can no longer be truncated to just the evolution of the conserved densities. Additional degrees of freedom play a significant role, and appear as additional poles of the retarded Green's function with lifetimes comparable to those of the hydrodynamic modes. (They may also manifest themselves as branch cuts, as is the case in some weakly coupled quantum field theories [17–19].) In cases where the density response exhibits a parametrically slow mode arising due to a weakly broken symmetry, the breakdown of hydrodynamics manifests itself as a collision in the complex frequency plane at nonzero wave vector k_{eq} between the hydrodynamic mode and the slow mode. In this case, it is often possible to augment the hydrodynamic description to incorporate this slow mode [6,20–28]. But typically the modes relevant for the breakdown of hydrodynamics are not of this nature, and a more complete knowledge of a system's microscopic details is required to understand them.

In contrast to this, in the nonzero temperature quantum critical phases found near quantum phase transitions, transport properties are typically universal and are governed by scaling properties of the critical point [29]. We might then expect that the breakdown of hydrodynamics in a quantum critical phase displays a greater degree of universality. However, it is often challenging to calculate concrete observables beyond thermodynamics due to the lack of analytically tractable models without any simplifying limits, such as a large number of degrees of freedom.

In this work, we exploit gauge-gravity duality to address hydrodynamic transport and its breakdown in quantum critical phases. Gauge-gravity duality maps the late time dynamics of certain large N_c quantum field theories (where N_c is the rank of the gauge group) to theories of gravity with a negative cosmological constant [15,30,31]. The relaxation of conserved densities back to equilibrium is captured exactly by the evolution of perturbations of asymptotically anti–de Sitter (AdS) black holes, which can be studied to obtain a precise understanding of the breakdown of hydrodynamics and the modes responsible for it [32,33].

Even in the absence of a weakly broken symmetry, the breakdown of hydrodynamics can be characterized by an energy scale ω_{eq} and wave number k_{eq}, which are sensitive to the system's microscopic details. ω_{eq} and k_{eq} are defined as the absolute values of the complex frequency ω and complex wave number k at which the hydrodynamic pole of the retarded Green's function first collides with a nonhydrodynamic pole or branch point [34–37]. [A different mechanism for the breakdown of hydrodynamics arises when interactions between hydrodynamic modes are included, in the guise of a nonanalytic frequency dependence of the retarded Green's functions (see, e.g., Ref. [14] for a review). This mechanism is expected to be suppressed in the large N limit [38].] The convergence properties of the real-space hydrodynamic gradient expansion in the linear regime are governed by k_{eq} [39] (see Ref. [40] for a study of the convergence of nonlinear hydrodynamics in real time), which also coincides with the radius of convergence of the small-k expansion of the hydrodynamic dispersion relation $\omega_{\mathrm{hydro}}(k)$. See Refs. [41–44] for recent applications of this.

In this work, we study the breakdown of hydrodynamics in certain low-temperature (T) states dual to black holes with nearly extremal $\mathrm{AdS}_2 \times \mathfrak{R}^2$ near-horizon metrics. These are examples of quantum critical phases with an emergent scaling symmetry in time [45–48], which has been dubbed "semilocal quantum critical." Formally, this scaling symmetry corresponds to an infinite Lifshitz scaling exponent, $z = +\infty$: time scales but space does not. Such states are closely related to the Sachdev-Ye-Kitaev- (SYK) like models of electrons in strange metals, which are governed by the same type of infrared fixed point in the limit of large number of fermions and strong interactions [49–60]. (The dimensionless SYK coupling is the interaction strength over temperature, so strong interactions are equivalent to low temperatures.) Specifically, we study the AdS_4 neutral, translation-breaking black brane of Refs. [61,62] and the AdS_4-Reissner-Nordström (AdS_4-RN) black brane, and the breakdown of the hydrodynamics governing the diffusive transport of energy, charge, and momentum in their dual states. The states we are interested in do not include any slow modes in the sense described above. Instead, local equilibration is controlled by the intrinsic dynamics of the quantum critical degrees of freedom of $\mathrm{AdS}_2 \times \mathfrak{R}^2$. We identify simple, general results for the local equilibration scales ω_{eq} and k_{eq} and confirm that these also apply to the SYK chain model studied in Ref. [44] in the limit of strong interactions.

Our first result is that the breakdown is caused by modes associated to the AdS_2 region of the geometry, and as a consequence ω_{eq} is set by universal (i.e., infrared) data via

$$\omega_{\mathrm{eq}} \to 2\pi\Delta T \quad \text{as } T \to 0, \tag{1}$$

where Δ is the infrared scaling dimension of the least irrelevant operator that couples to the diffusion mode. This is in contrast to systems with a weakly broken symmetry, for which $\omega_{\mathrm{eq}} \ll T$, but is in line with the expectation that the quantum critical dynamics is controlled by a "Planckian" timescale $\tau_{\mathrm{eq}} \sim 1/T$ [29,63]. More precisely, we find that at small k and T the Fourier space locations of the longest-lived nonhydrodynamic poles are inherited from infrared Green's functions, and are approximately located at $\omega_n \equiv -i(n+\Delta)2\pi T$ for non-negative integers n. The breakdown is characterized by a collision, parametrically close to the imaginary ω axis, between the $n = 0$ mode (which has a weak k dependence) and the hydrodynamic mode. This collision manifests itself as a branch-point singularity in the dispersion relation of the mode.

Secondly, we find that at low temperatures the corrections to the quadratic approximation $-iDk^2$ to the exact hydrodynamic dispersion relation are parametrically small such that the collision occurs when k is almost real and

$$k_{\mathrm{eq}}^2 \to \frac{\omega_{\mathrm{eq}}}{D} \quad \text{as } T \to 0. \tag{2}$$

In other words, the scales k_{eq} and ω_{eq} governing the regime of validity of hydrodynamics are set simply by the diffusivity D and the scaling dimension Δ. In some of the examples we study (those involving diffusion of energy), the relevant diffusivity is controlled by an irrelevant deformation of the AdS_2 fixed point and in these cases the result (2) indicates that k_{eq} is controlled by the same irrelevant deformation. *A priori*, the result (2) is quite surprising: it relates the radius of convergence to just the leading-order term in the hydrodynamic expansion. This is a consequence of the AdS_2 fixed point.

By rearranging Eq. (2) we obtain an answer to the question raised in Ref. [7] of what the underlying velocity and timescales are that govern the diffusivity in non-quasiparticle systems. In all our examples they are set by the local equilibration scales,

$$D \to v_{eq}^2 \tau_{eq} \quad \text{as } T \to 0, \tag{3}$$

where $v_{eq} \equiv \omega_{eq}/k_{eq}$ and $\tau_{eq} \equiv \omega_{eq}^{-1}$ are the velocity and timescale associated to local equilibration.

In the cases where diffusive hydrodynamics breaks down due to a parametrically slow mode protected by a weakly broken symmetry, D is typically set by τ_{eq} and the speed of the propagating mode that dominates following the breakdown [64]. We emphasize that the breakdown of hydrodynamics is qualitatively different in the cases we study: there is not a single slow mode but a tower of AdS_2 modes with parametrically similar lifetimes set by ω_n, and the breakdown does not produce a propagating mode with velocity $v \simeq v_{eq}$. More generally, the local equilibration time has been argued to set an upper bound on the diffusivity in Refs. [65,66]. All examples that we study are consistent with a bound of the form $D \lesssim v_{eq}^2 \tau_{eq}$ for the range of parameters we have investigated.

In the absence of a slow mode, it was proposed that low-temperature diffusivities are set by the butterfly velocity v_B and Lyapunov time τ_L that characterize the onset of scrambling following thermalization of the system [67]. This was shown to robustly apply to the diffusivity of energy density D_ε in holographic theories and SYK-like models [58,59,68–71]. For the examples we study, $\tau_L^{-1} = 2\pi T$ and

$$D_\varepsilon \to v_B^2 \tau_L \quad \text{as } T \to 0, \tag{4}$$

which is furthermore true in general for states governed by an infrared AdS_2 with the universal deformation [69].

As for our result (3), Eq. (4) can be viewed as a consequence of the excellent applicability of the quadratic approximation to the exact hydrodynamic dispersion relation up to the relevant scale. Specifically, pole-skipping analysis suggests that the energy diffusion mode satisfies $\omega_{\text{hydro}}(k = i v_B^{-1} \tau_L^{-1}) = i \tau_L^{-1}$ [72–74], from which Eq. (4) follows assuming corrections to the quadratic, diffusive form $-iD_\varepsilon k^2$ at $k = i v_B^{-1} \tau_L^{-1}$ are parametrically small as $T \to 0$.

Our result (3) is more general than Eq. (4) in that it is true for all diffusivities in the examples we study, not just the diffusion of energy. Fundamentally this is because, by definition, all diffusive modes pass through the location set by (ω_{eq}, k_{eq}), while only the energy diffusion mode satisfies the pole-skipping constraint above [75]. As a consequence we provide a new perspective on, and generalization of, the relations between equilibration, transport, and scrambling and their applications in AdS_2- and SYK-like models of electrons in strange metals.

In the remainder of this work we explain how we arrive at Eqs. (1) and (2) before closing with comments on implications and the more general applicability of our results. Technical details of our calculations are presented in Supplemental Material [76].

II. DIFFUSIVE HYDRODYNAMICS

The spectrum of hydrodynamic modes is dependent on the system under consideration, and by our definition each hydrodynamic mode has its own associated local equilibration scales ω_{eq} and k_{eq}. We focus on hydrodynamic diffusion modes, which arise when a system has a current density j with constitutive relation

$$j(\rho) = -D_\rho \nabla\rho + O(\nabla^3), \tag{5}$$

where ρ is the corresponding conserved density. ρ will then obey the diffusion equation with diffusivity D_ρ at leading order in the derivative expansion, and has a retarded Green's function [14,16],

$$G_{\rho\rho}(\omega, k) = \frac{D_\rho \chi_{\rho\rho} k^2 + \cdots}{-i\omega + D_\rho k^2 + \cdots}, \tag{6}$$

where $\chi_{\rho\rho} \equiv \lim_{\omega\to 0} G_{\rho\rho}(\omega, k)$ is the static susceptibility of ρ, and ellipses denote terms with higher powers of ω and k. The dispersion relation of the hydrodynamic diffusion mode is then

$$\omega_{\text{hydro}}(k) = -iD_\rho k^2 + O(k^4). \tag{7}$$

Hydrodynamic diffusion is a very general phenomenon. Even within the restricted class of systems that we study, the set of conserved densities that exhibit hydrodynamic diffusion varies. In this work, we are interested in the diffusion of energy ε and of transverse momentum Π.

III. DIFFUSION IN A NEUTRAL HOLOGRAPHIC STATE

We begin with the AdS_4 neutral translation-breaking model [61,62] which is a classical solution of the action

$$S = \int d^4x\sqrt{-g}\left(\mathfrak{R} + 6 - \frac{1}{2}\sum_{i=1}^{2}(\partial\varphi_i)^2\right), \tag{8}$$

with spacetime metric,

$$ds^2 = -r^2 f(r)dt^2 + r^2 \underline{dx}^2 + \frac{dr^2}{r^2 f(r)}, \tag{9}$$

supported by two scalar fields $\varphi_i = mx^i$ $(i = 1, 2)$ that break translational symmetry. The emblackening factor of the solution is

$$f(r) = 1 - \frac{m^2}{2r^2} - \left(1 - \frac{m^2}{2r_0^2}\right)\frac{r_0^3}{r^3}, \tag{10}$$

where r_0 denotes the location of the horizon with associated temperature T. The linear perturbations can be written in terms of four decoupled variables and we focus on the one exhibiting the single hydrodynamic mode of the system. See Ref. [76] for further details on this spacetime, and on the calculations leading to the results below.

A. Hydrodynamic mode

The hydrodynamic mode corresponds to diffusion of energy, with the small k dispersion relation (7) and diffusivity $D_\varepsilon \to \sqrt{3/2}m^{-1}$ in the low-T limit [20].

First, we quantify corrections to this result that will enable us to understand the breakdown of hydrodynamics. In the low-temperature limit $T \sim k^2 \sim \epsilon \ll 1$, the retarded Green's function of energy density $G_{\varepsilon\varepsilon}$ exhibits a pole located at

$$\omega(k) = -i\epsilon\sqrt{\frac{3}{2}}\frac{k^2}{m}\left[1 + \epsilon\frac{k^2}{m^2} + \epsilon^2\left(\frac{4\pi T^2}{3m^2} + \frac{k^4}{m^4}\right) + \cdots\right], \tag{11}$$

where we have explicitly written all ϵ dependence. For suitably small k, this is an approximation to the dispersion relation of the hydrodynamic mode as we show in Fig. 1. It becomes invalid near specific wave numbers $k^2 = k_n^2$ related to the breakdown of hydrodynamics, which we address shortly.

It is important to note that Eq. (11) is different than the hydrodynamic expansion: corrections to the quadratic k^2 term are not being neglected as in the usual gradient expansion, but are parametrically small in this limit under consideration. One consequence of this is that if we define any wave number k_* with $k_*^2 \sim T$ at low T, and define ω_* to be the location of the hydrodynamic pole at this wave number, then Eq. (11) implies $D_\varepsilon \to i\omega_*/k_*^2$ as $T \to 0$. For example, choosing $k_* = iv_B^{-1}\tau_L^{-1}$ results in the chaos relation (4) as described in Sec. I. (See Fig. 2 of Ref. [74] for a visual representation of this.)

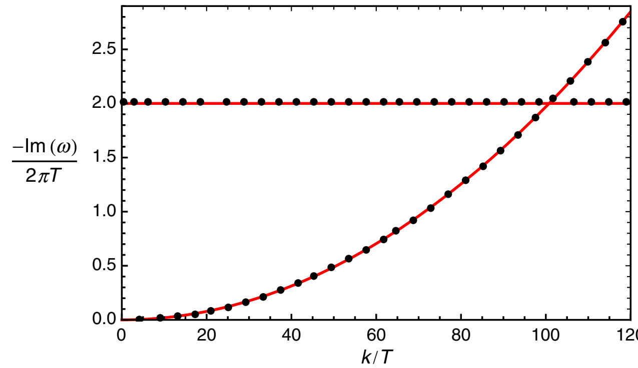

FIG. 1. Frequencies of the hydrodynamic and longest-lived infrared modes at $T/m = 10^{-3}$. Black circles are numerical results and red lines are the analytic expressions (11) and (13). For real k, all poles displayed have purely imaginary frequencies.

We soon show that the breakdown of hydrodynamics at low T is characterized by a pole collision at $k_{\rm eq}^2 \sim T$, $\omega_{\rm eq} \sim T$ and thus the diffusivity can alternatively be expressed simply in terms of these scales by Eq. (2). But prior to exploring the pole collision that characterizes the breakdown of hydrodynamics, it is instructive to first understand the origin of the nonhydrodynamic mode responsible.

B. Infrared modes

At low T the state is governed by an infrared fixed point manifest in the emergence of a near-horizon $AdS_2 \times \mathfrak{R}^2$ metric with special linear group [SL(2,R)] symmetry (see Ref. [76]). Each linear perturbation of the spacetime can be characterized by $\Delta(k)$, a wave-number-dependent scaling dimension of the corresponding operator with respect to this infrared fixed point, and a corresponding infrared Green's function [47,83],

$$\mathcal{G}_{\rm IR} \propto T^{2\Delta(k)-1}\frac{\Gamma[\frac{1}{2} - \Delta(k)]\Gamma[\Delta(k) - \frac{i\omega}{2\pi T}]}{\Gamma[\frac{1}{2} + \Delta(k)]\Gamma[1 - \Delta(k) - \frac{i\omega}{2\pi T}]}. \tag{12}$$

For the spacetime perturbation that exhibits a diffusive mode, $\Delta(k) = (1 + \sqrt{9 + 8k^2/m^2})/2$.

Although analytically reconstructing $G_{\varepsilon\varepsilon}$ from $\mathcal{G}_{\rm IR}$ is not easy, for our purposes it is enough to observe that $G_{\varepsilon\varepsilon}$ exhibits poles whose locations approach those of the poles of $\mathcal{G}_{\rm IR}$ as $k, T \to 0$. Specifically, this means that in this limit $G_{\varepsilon\varepsilon}$ exhibits poles at

$$\omega \to \omega_n = -i2\pi T[n + \Delta(0)], \quad n = 0, 1, 2, \ldots, \tag{13}$$

with $\Delta(0) = 2$. The dispersion relation of the $n = 0$ pole is shown in Fig. 1.

At low T, the infrared modes Eq. (13) have a parametrically longer lifetime than the other nonhydrodynamic

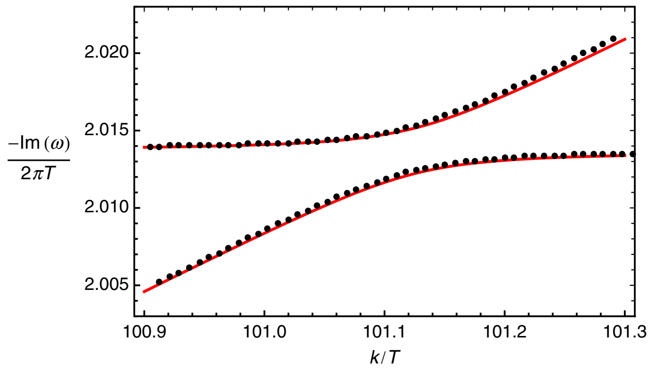

FIG. 2. Frequencies of the hydrodynamic and longest-lived infrared modes at $T/m = 10^{-3}$, enlarging the region near ω_0. The black dots are the numerical results (the bottom dots are the hydrodynamic mode, the top ones the longest-lived nonhydrodynamic mode), the red lines show the dispersion relations extracted analytically from Eq. (14) for real values of k. The pole collision is not visible here as it happens at a complex value of k.

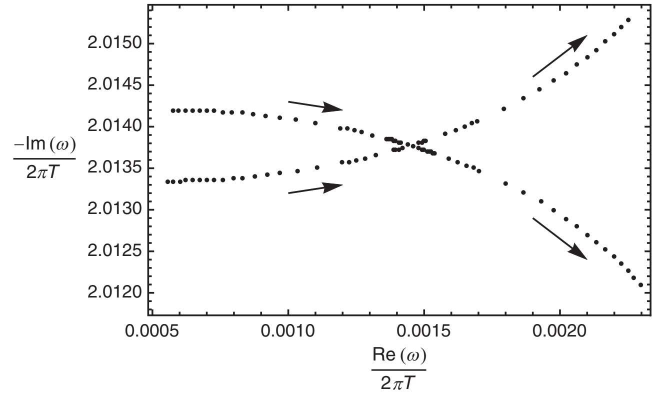

FIG. 3. Motion of the hydrodynamic (starting in the bottom left of the plot) and longest-lived infrared mode (starting in the top left of the plot) in the complex ω plane as $|k|/T$ is increased (from approximately 101.09 to approximately 101.15) at fixed $T/m = 10^{-3}$ and fixed phase of the wave number $\phi_k \simeq 7.095 \times 10^{-4}$. There is a collision for $|k| \simeq 101.120T$. Equation (14) predicts a collision at $|k| \simeq 101.125T$ and $\phi_k \simeq 7.374 \times 10^{-4}$. In Fig. S2 in Ref. [76], we show that the discrepancy between the numerical and analytical values from Eq. (14) decreases with temperature.

poles of $G_{\varepsilon\varepsilon}$, and are responsible for the breakdown of hydrodynamics.

The wave numbers at which our calculation of the low-T dispersion relation (11) of the hydrodynamic mode is invalid are $k_n^2 = \sqrt{8/3}(2+n)\pi m T + O(T^2)$ [see Eq. (43) of Ref. [76] for a precise expression for k_n], for which the mode would be located at precisely $\omega(k_n) = \omega_n$ in the limit of low T. The natural interpretation would therefore be that the invalidity of the calculation at these values of k^2 can be traced to the nearby presence of the infrared mode (assuming that the location of the infrared mode has a weak k dependence). A more refined calculation below confirms this, as well as the existence of a collision between these modes for complex k that signals the breakdown of hydrodynamics.

C. Breakdown of hydrodynamics

In order to extract the existence of the pole collision, a more refined perturbative computation of $G_{\varepsilon\varepsilon}$ at the points $\omega = \omega_n + \delta\omega, k^2 = k_n^2 + \delta(k^2)$ is required. This yields

$$G_{\varepsilon\varepsilon}^{-1}(\omega, k) \propto [\mathcal{D}_n \delta(k^2) - i\delta\omega](1 - i\tau_n\delta\omega) - i\lambda_n\delta\omega, \qquad (14)$$

where we show only terms relevant for understanding the collision. The low-T limit of each coefficient is

$$\tau_n \to \frac{9m}{16\sqrt{6}(2+n)\pi^2 T^2}, \qquad \lambda_n \to \sqrt{\frac{3}{2}}[n(n+4)+3]\frac{\pi T}{m}, \qquad (15)$$

while $\mathcal{D}_n \to D_\varepsilon$ in the same limit. The comparable size of the $\delta\omega$ and $\tau_n(\delta\omega)^2$ terms at frequencies $\delta\omega \sim T^2$ indicates that for such frequencies $G_{\varepsilon\varepsilon}$ is dominated by two poles, whose dispersion relations are given by solving the quadratic equation (14) for $\delta\omega(\delta k)$. In Fig. 2 we show that indeed Eq. (14) correctly describes the locations of the two poles near ω_0 for real values of k, including the absence of a collision. The poles collide (coincide in Fourier space) at the complex value of δk where the discriminant of the quadratic polynomial vanishes, and the dispersion relation has a branch point. This collision is shown in Fig. 3.

The collision closest to the origin of k space ($n = 0$) signals the breakdown of hydrodynamics. The absolute values of k and ω at this collision are (as $T \to 0$)

$$\omega_{\mathrm{eq}} \equiv |\omega_{\mathrm{collision}}| \to 4\pi T\left(1 + \frac{8\sqrt{6}\pi T}{9m} + \cdots\right),$$
$$k_{\mathrm{eq}}^2 \equiv |k_{\mathrm{collision}}|^2 \to \frac{\omega_{\mathrm{eq}}}{D_\varepsilon}\left(1 - \frac{4\sqrt{6}\pi T}{3m} + \cdots\right), \qquad (16)$$

from which our main results (1) and (2) follow.

The collision location asymptotically approaches real (imaginary) values of k (ω) as $T \to 0$. More precisely, as $T \to 0$ the phases of k and ω at the collision point are

$$\phi_k \to \frac{2^4}{6^{3/4}}\left(\frac{\pi T}{m}\right)^{3/2}, \qquad \phi_\omega \to -\frac{\pi}{2} + \phi_k, \qquad (17)$$

where $k_{\mathrm{collision}} = k_{\mathrm{eq}} e^{i\phi_k}$ and $\omega_{\mathrm{collision}} = \omega_{\mathrm{eq}} e^{i\phi_\omega}$.

Note that even after the pole collision formally indicating the breakdown of hydrodynamics, Fig. 4 illustrates that the system continues to exhibit a diffusionlike mode described extremely well by the dispersion relation (11). In the limit of zero temperature, the tower of infrared poles in $\mathrm{AdS}_2 \times \mathfrak{R}^2$ coalesces in a branch cut along the imaginary axis [47,84]. As the branch cut passes through $k = 0$, we expect that a hydrodynamiclike series for the dispersion relation at

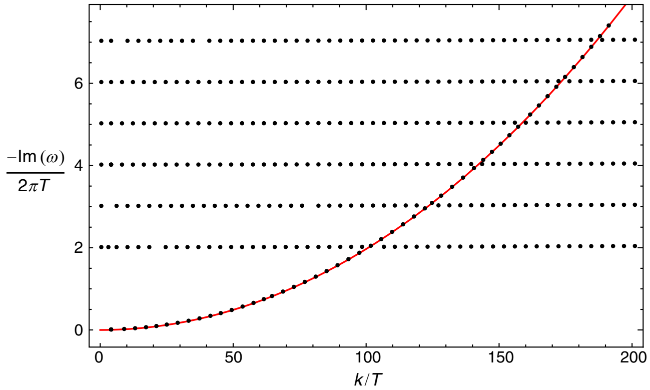

FIG. 4. Numerical results for the frequencies of the hydrodynamic and longest-lived infrared modes of the neutral, translation-symmetry breaking model at $T/m = 10^{-3}$ (circles). Away from $\omega_{n\geq 0}$, the analytic dispersion relation (11) (solid red line) provides an excellent approximation to the exact location of a pole.

$T = 0$ would contain nonanalytic terms, as was found recently in Ref. [85] for a similar state.

IV. DIFFUSION IN A CHARGED HOLOGRAPHIC STATE

The AdS_4-RN solution to Einstein-Maxwell gravity,

$$S = \int d^4x\sqrt{-g}\left(\mathfrak{R} + 6 - \frac{1}{4}F^2\right), \tag{18}$$

has a metric of the form Eq. (9) but supported by a radial electric field,

$$A_t = \mu\left(1 - \frac{r_0}{r}\right), \tag{19}$$

such that the emblackening factor is

$$f(r) = 1 - \left(1 + \frac{\mu^2}{4r_0^2}\right)\frac{r_0^3}{r^3} + \frac{\mu^2 r_0^2}{4r^4}. \tag{20}$$

This solution represents a translationally invariant state with $U(1)$ chemical potential μ, and its linear perturbations can be written in terms of four decoupled variables. Further details of the solution and the calculations underlying our results are given in Ref. [76].

The state exhibits two independent diffusive hydrodynamic modes, each associated to a different such variable. The first, corresponding to diffusion of energy and $U(1)$ charge with diffusivity D_ε, is analogous to the diffusive mode of the previous section. (In the low-T limit both such modes have $D_\varepsilon = \kappa/c_\rho$ with κ the open circuit thermal conductivity and c_ρ the heat capacity [28,69].) The second corresponds to the transverse diffusion of momentum with diffusivity D_Π. In the limit of low temperature, the diffusivities are (see Ref. [76] for the full, T-dependent expressions)

$$D_\varepsilon(T=0) = \frac{\sqrt{3}}{\mu}, \qquad D_\Pi(T=0) = \frac{1}{\sqrt{12}\mu}. \tag{21}$$

The variables exhibiting each of these modes have $k \to 0$ infrared scaling dimensions [84,86,87],

$$\Delta_\varepsilon(0) = 2, \qquad \Delta_\Pi(0) = 1, \tag{22}$$

and numerical calculations confirm that at small k and T each corresponding retarded Green's function exhibits nonhydrodynamic poles at the locations (13). As before, a collision close to the imaginary ω axis between the longest-lived such pole and the hydrodynamic pole signifies the independent breakdown of hydrodynamics in each case.

At low T (and until the collision occurs) both hydrodynamic modes are described extremely well by the quadratic approximation to the hydrodynamic dispersion relation, while the locations of the longest-lived nonhydrodynamic poles depend only very weakly on k. As a consequence, the equilibration scales in both cases are set by the simple formulas (1) and (2) as shown in Fig. 5.

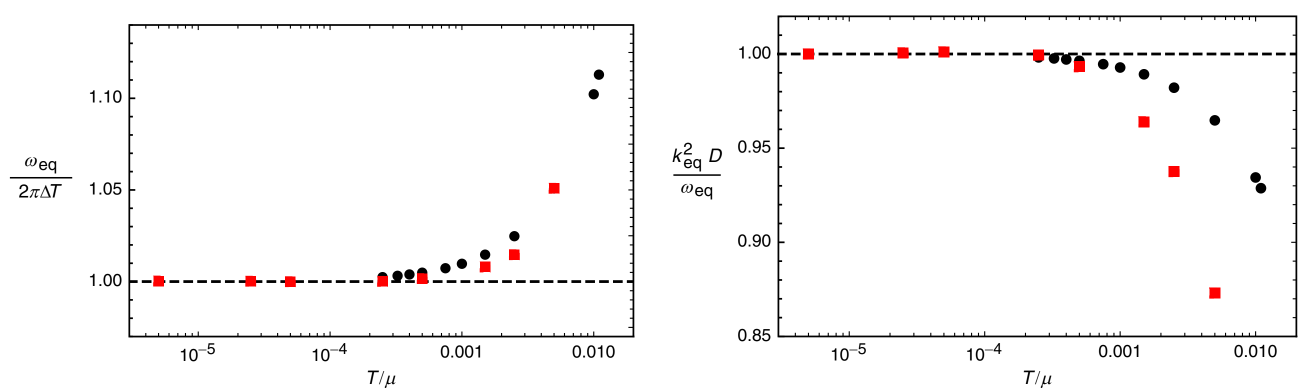

FIG. 5. Numerically obtained local equilibration data for diffusive hydrodynamics in $G_{\varepsilon\varepsilon}$ (black circles) and $G_{\Pi\Pi}$ (red squares) of the charged state.

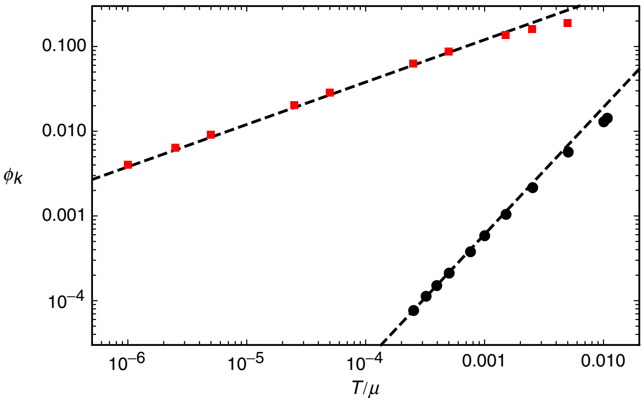

FIG. 6. Numerically obtained ϕ_k for $G_{\varepsilon\varepsilon}$ (black circles) and $G_{\Pi\Pi}$ (red squares) of the charged state. Dashed lines shows the best fits to a power law at small T: $\phi_k = 19.2(T/\mu)^{1.50}$ and $\phi_k = 3.80(T/\mu)^{0.50}$, respectively.

The phase of the collision wave number ϕ_k in each case is shown in Fig. 6, illustrating that the collision point asymptotically approaches real values of k as $T \to 0$. Both cases here, and the result (17) in the previous example, are consistent with Δ controlling the low-T scaling of the phase via $\phi_k \sim T^{\Delta - 1/2}$.

As in the previous example, the system continues to exhibit diffusionlike modes even after the collision formally indicating the breakdown of hydrodynamics. The dispersion relations of these modes are extremely well approximated by the quadratic approximation to diffusive hydrodynamics, as shown in Fig. S3 of Ref. [76].

V. COMPARISON WITH SYK CHAIN

The SYK model is a $(0+1)$-dimensional theory of N interacting fermions that, in the limit of large N and strong interactions, is governed by the same effective action as a theory of gravity in a nearly-AdS_2 spacetime [49–57]. The SYK chain [58] is a higher-dimensional generalization of this, which has served as a very useful toy model for studying diffusive energy transport in strange metal states of matter. As it exhibits the local quantum criticality characteristic of $\mathrm{AdS}_2 \times \mathfrak{R}^2$ fixed points, it is natural to ask whether local equilibration in this explicit microscopic model is governed by our general results (1) and (2).

In Ref. [44], a SYK chain model with N Majorana fermions per site $\chi_{i,x}$ and Hamiltonian

$$H = i^{q/2} \sum_{x=0}^{M-1} \Bigg(\sum_{1 \le i_1 < \cdots < i_q \le N} J_{i_1 \ldots i_q, x} \chi_{i_1, x} \cdots \chi_{i_q, x} + \sum_{\substack{1 \le i_1 < \cdots < i_{q/2} \le N \\ 1 \le j_1 < \cdots < j_{q/2} \le N}} J'_{i_1 \ldots i_{q/2} j_1 \ldots j_{q/2}, x} \chi_{i_1, x} \cdots \chi_{i_{q/2}, x} \chi_{j_1, x+1} \cdots \chi_{j_{q/2}, x+1} \Bigg) \tag{23}$$

was studied. The two terms represent q-body on-site and nearest-neighbor interactions, respectively, where the couplings $J_{i_1 \ldots i_q, x}$ and $J'_{i_1 \ldots i_{q/2} j_1 \ldots j_{q/2}, x}$ are Gaussian random variables with zero mean. Remarkably, in the limit $N \gg q^2 \gg 1$ an exact analytic expression for $G_{\varepsilon\varepsilon}$ was found for all values of the effective interaction strength $0 < v < 1$ and the relative strength of on-site and intersite interactions $0 < \gamma \le 1$ [44]. The analytic expression is given in Ref. [76], where the details of the model are also summarized.

Taking advantage of this result, a detailed study of the breakdown of diffusive hydrodynamics as a function of interaction strength v was performed in Ref. [44]. Here we focus on the limit of strong interactions $v \to 1$, which is equivalent to $T \to 0$. In this limit, the longest-lived nonhydrodynamic modes are a series of infrared modes located at precisely the frequencies ω_n of Eq. (13) with $\Delta = 2$ as $k \to 0$. Hydrodynamics breaks down due to a collision between the hydrodynamic mode and the longest-lived of these infrared modes, and in Fig. 7 we confirm that the local equilibration scales are given simply by

$$\omega_{\mathrm{eq}} \to 2\pi\Delta T \quad \text{and} \quad k_{\mathrm{eq}}^2 \to \frac{\omega_{\mathrm{eq}}}{D_\varepsilon} \quad \text{as } v \to 1, \tag{24}$$

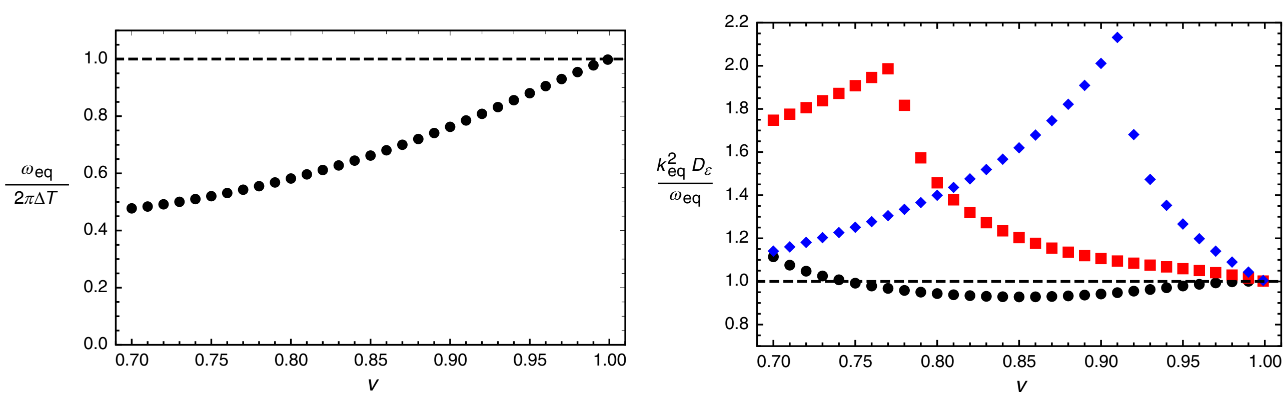

FIG. 7. Local equilibration frequency (left) and diffusivity ratio (right) for the large-q SYK chain model. ω_{eq} is γ independent, while the diffusivity ratio is shown for $\gamma = 1$ (black circles), $\gamma = 0.4$ (red squares), and $\gamma = 0.2$ (blue diamonds).

analogously to Eqs. (1) and (2). Unlike in the holographic examples, the pole collision at strong interactions here happens for real k (i.e., $\phi_k = 0$). It would be interesting to determine whether finite $1/q$ corrections generate a small nonzero phase ϕ_k. Consistently with the other examples we have presented, following the formal breakdown of hydrodynamics the spectrum still contains a mode whose dispersion relation is very well approximated by the quadratic approximation to diffusive hydrodynamics.

VI. OUTLOOK

There is good reason to expect that at least some of our results will generalize beyond the specific examples studied here to other states governed by AdS_2 infrared fixed points. While our key observation that the quadratic approximation to the hydrodynamic dispersion relation works parametrically well even for wave numbers $k^2 \sim T$ seems unusual, it is nontrivially consistent with the result (4) that is indeed true for holographic $\mathrm{AdS}_2 \times \mathfrak{R}^2$ fixed points with a universal deformation [69] as well as in related SYK chain models [58,59].

There are more general holographic and SYK-like systems governed by AdS_2 fixed points that exhibit additional diffusive modes beyond the two types we have studied. Of particular interest are nontranslationally invariant systems with a $U(1)$ symmetry, for which an Einstein relation relates the electrical resistivity to a diffusivity [7,59,69]. If our results (1) and (2) extend to such modes, they will therefore also provide a simple relation between the phenomenologically important electrical resistivity and the local equilibration scales of such strongly correlated systems.

Confirmation of the broader applicability of our result (3) for $\mathrm{AdS}_2 \times \mathfrak{R}^2$ solutions would be an important step for quantifying diffusivities near general infrared fixed points. One way to do this would be to identify a speed u and timescale τ such that in general $D \sim u^2\tau$ with the coefficient being T independent. This is difficult even for the relatively simple case of holographic energy diffusion, primarily because there are two exceptional types of fixed point where dangerously irrelevant deformations take over the properties of the mode: $\mathrm{AdS}_2 \times \mathfrak{R}^2$ fixed points (i.e., dynamical critical exponent $z = \infty$) [69] and relativistic fixed points (i.e., $z = 1$) [70]. If our result does generalize to $\mathrm{AdS}_2 \times \mathfrak{R}^2$ solutions (including those with nonuniversal deformations), both of these exceptional cases will be consistent with the identification $u = v_{\mathrm{eq}}$ and $\tau = \tau_{\mathrm{eq}}$ (we expect the result of Ref. [64] to apply to the $z = 1$ cases due to the existence of a parametrically slow mode [26,28]; see also Ref. [88]). Provided that naive T scaling holds for the equilibration scales in the other cases with finite Lifshitz exponent z ($\tau_{\mathrm{eq}} \sim 1/T$ and $v_{\mathrm{eq}} \sim T^{1-1/z}$), which seems likely, this identification will then work for all fixed points.

For cases where the breakdown of hydrodynamics is due to a slow mode, it is the separation of scales between the decay rate of the slow mode Γ and that of typical nonhydrodynamic excitations T that allows one to augment the hydrodynamic description to incorporate the slow mode. Mathematically, the separation allows one to resum the hydrodynamic expansion into a square root form, valid at scales $\omega \sim k \sim \Gamma$ (see, e.g., Refs. [20,25,27]). This makes manifest the convergence properties of the hydrodynamic expansion, $k_{\mathrm{eq}} \sim \Gamma$. It would be very interesting if one could extract an analogous effective theory for the cases described here, taking advantage of the separation of scales between the decay rate of the infrared modes (set by T) and that of the other nonhydrodynamic excitations (set by the curvature of AdS_2). Such an effective theory would need to resum the effects of the entire tower of infrared modes and would give a greater understanding of why the quadratic approximation to diffusive hydrodynamics is valid up to (and indeed beyond) the wave number k_{eq}.

It would also be interesting to study whether our results continue to hold for AdS_2 fixed points supported by a different hierarchy of scales (such as large angular momentum or magnetic field compared to temperature), and whether analogous results hold for other types of hydrodynamic modes near these fixed points.

It would be very useful to have a semiholographic description of our results (along the lines of Refs. [91,92]), in which we couple a gapless hydrodynamic diffusion mode to the tower of infrared modes associated with the AdS_2 region of the spacetime. Our results rely on the fact that the two types of mode have very little effect on one another (see, e.g., Fig. 1) and a semiholographic description may clarify exactly under what conditions this is the case. A related avenue would be to adapt the recently constructed holographic effective Schwinger-Keldysh action for diffusion to AdS_2 horizons [92–95].

Extending our work to Schrödinger $z = 2$ IR geometries would allow us to make contact with ultracold atomic systems [96], which realize a strongly interacting Fermi gas near unitarity [5].

In Ref. [97], the charge diffusivity of a cold atomic system coupled to an optical lattice was measured. In Refs. [98,99], the thermal diffusivity of high-T_c superconductors in the strange metallic regime was also reported. It would be interesting to investigate the deviations from diffusive hydrodynamics in these systems.

The examples we studied are all consistent with bounds on D of the type proposed in Refs. [65,66] but with the velocity in the bound given by v_{eq} (rather than the operator growth velocity, characteristic velocity of low-energy excitations, or butterfly velocity). (While the SYK chain results shown in Fig. 7 do not obey a strict bound $D \leq v_{\mathrm{eq}}^2\tau_{\mathrm{eq}}$, there is no parametric violation of such a relation and thus they are consistent with Refs. [65,66].) Indeed, the arguments in Refs. [65,66] assume that v_{eq} is set by one of these velocities and thus imply the bound $D \lesssim v_{\mathrm{eq}}^2 \tau_{\mathrm{eq}}$. In this sense our results support the assumption of Refs. [65,66] that the local equilibration is controlled by an underlying effective light cone, even though the systems are nonrelativistic. It would be very worthwhile to determine D, v_{eq}, and τ_{eq} for other states, and over a wider parameter range, in order to establish the robustness of these observations and to determine whether v_{eq} is set by a speed such as the butterfly velocity in general.

ACKNOWLEDGMENTS

We are grateful to Changha Choi, Luca Delacrétaz, Sašo Grozdanov, Sean Hartnoll, Márk Mezei, Subir Sachdev, Gábor Sárosi, and Benjamin Withers for helpful discussions. D. A. is supported by the "Atracción de Talento" program (2017-T1/TIC-5258, Comunidad de Madrid), the Severo Ochoa Excellence Grant No. SEV-2016-0597592 from the Ministerio de Ciencia e Innovación and the Grant No. PGC2018-095976-B-C21 from the MINECO. The work of R. A. D. is supported by the STFC Ernest Rutherford Grant No. ST/R004455/1. The work of B. G. is supported by the European Research Council (ERC) under the European Union's Horizon 2020 research and innovation program (Grant Agreement No. 758759). The work of K. S. is supported by the European Research Council (ERC) under the European Union's Horizon 2020 research and innovation program (Grants Agreement No. 758759 and No. 818066).

[1] P. K. Kovtun, D. T. Son, and A. O. Starinets, *Viscosity in Strongly Interacting Quantum Field Theories from Black Hole Physics*, Phys. Rev. Lett. **94**, 111601 (2005).

[2] M. P. Heller, *Holography, Hydrodynamization and Heavy-Ion Collisions*, Acta Phys. Pol. B **47**, 2581 (2016).

[3] P. Romatschke, *Do Nuclear Collisions Create a Locally Equilibrated Quark–Gluon Plasma?*, Eur. Phys. J. C **77**, 21 (2017).

[4] J. Berges, M. P. Heller, A. Mazeliauskas, and R. Venugopalan, *Thermalization in QCD: Theoretical Approaches, Phenomenological Applications, and Interdisciplinary Connections*, arXiv:2005.12299.

[5] T. Enss and J. H. Thywissen, *Universal Spin Transport and Quantum Bounds for Unitary Fermions*, Annu. Rev. Condens. Matter Phys. **10**, 85 (2019).

[6] S. A. Hartnoll, P. K. Kovtun, M. Muller, and S. Sachdev, *Theory of the Nernst Effect near Quantum Phase Transitions in Condensed Matter, and in Dyonic Black Holes*, Phys. Rev. B **76**, 144502 (2007).

[7] S. A. Hartnoll, *Theory of Universal Incoherent Metallic Transport*, Nat. Phys. **11**, 54 (2015).

[8] L. Levitov and G. Falkovich, *Electron Viscosity, Current Vortices and Negative Nonlocal Resistance in Graphene*, Nat. Phys. **12**, 672 (2016).

[9] D. A. Bandurin, I. Torre, R. K. Kumar, M. B. Shalom, A. Tomadin, A. Principi, G. H. Auton, E. Khestanova, K. S. Novoselov, I. V. Grigorieva *et al.*, *Negative Local Resistance Caused by Viscous Electron Backflow in Graphene*, Science **351**, 1055 (2016).

[10] J. Crossno, J. K. Shi, K. Wang, X. Liu, A. Harzheim, A. Lucas, S. Sachdev, P. Kim, T. Taniguchi, K. Watanabe *et al.*, *Observation of the Dirac Fluid and the Breakdown of the Wiedemann-Franz Law in Graphene*, Science **351**, 1058 (2016).

[11] P. J. W. Moll, P. Kushwaha, N. Nandi, B. Schmidt, and A. P. Mackenzie, *Evidence for Hydrodynamic Electron Flow in* $PdCoO_2$, Science **351**, 1061 (2016).

[12] A. Lucas and K. C. Fong, *Hydrodynamics of Electrons in Graphene*, J. Phys. Condens. Matter **30**, 053001 (2018).

[13] D. Forster, *Hydrodynamic Fluctuations, Broken Symmetry, and Correlation Functions*, Frontiers in Physics Vol. 47 (W.A. Benjamin, Inc., Reading, MA, 1975), p. 343.

[14] P. Kovtun, *Lectures on Hydrodynamic Fluctuations in Relativistic Theories*, J. Phys. A **45**, 473001 (2012).

[15] S. A. Hartnoll, A. Lucas, and S. Sachdev, *Holographic Quantum Matter* (MIT Press, Cambridge, MA, 2018).

[16] L. P. Kadanoff and P. C. Martin, *Hydrodynamic Equations and Correlation Functions*, Ann. Phys. (N.Y.) **281**, 800 (2000).

[17] S. A. Hartnoll and S. Kumar, *AdS Black Holes and Thermal Yang-Mills Correlators*, J. High Energy Phys. 12 (2005) 036.

[18] P. Romatschke, *Retarded Correlators in Kinetic Theory: Branch Cuts, Poles and Hydrodynamic Onset Transitions*, Eur. Phys. J. C **76**, 352 (2016).

[19] A. Kurkela and U. A. Wiedemann, *Analytic Structure of Nonhydrodynamic Modes in Kinetic Theory*, Eur. Phys. J. C **79**, 776 (2019).

[20] R. A. Davison and B. Goutéraux, *Momentum Dissipation and Effective Theories of Coherent and Incoherent Transport*, J. High Energy Phys. 01 (2015) 039.

[21] A. Lucas, *Conductivity of a Strange Metal: From Holography to Memory Functions*, J. High Energy Phys. 03 (2015) 071.

[22] A. Lucas, *Hydrodynamic transport in strongly coupled disordered quantum field theories*, New J. Phys. **17**, 113007 (2015), arXiv:1506.02662.

[23] R. A. Davison, L. V. Delacrétaz, B. Goutéraux, and S. A. Hartnoll, *Hydrodynamic Theory of Quantum Fluctuating Superconductivity*, Phys. Rev. B **94**, 054502 (2016); Phys. Rev. B **96**, 059902(E) (2017).

[24] L. V. Delacrétaz, B. Goutéraux, S. A. Hartnoll, and A. Karlsson, *Theory of Hydrodynamic Transport in Fluctuating Electronic Charge Density Wave States*, Phys. Rev. B **96**, 195128 (2017).

[25] C.-F. Chen and A. Lucas, *Origin of the Drude Peak and of Zero Sound in Probe Brane Holography*, Phys. Lett. B **774**, 569 (2017).

[26] R. A. Davison, S. A. Gentle, and B. Goutéraux, *Slow Relaxation and Diffusion in Holographic Quantum Critical Phases*, Phys. Rev. Lett. **123**, 141601 (2019).

[27] S. Grozdanov, A. Lucas, and N. Poovuttikul, *Holography and Hydrodynamics with Weakly Broken Symmetries*, Phys. Rev. D **99**, 086012 (2019).

[28] R. A. Davison, S. A. Gentle, and B. Goutéraux, *Impact of Irrelevant Deformations on Thermodynamics and*

Transport in Holographic Quantum Critical States, Phys. Rev. D **100**, 086020 (2019).
[29] S. Sachdev, *Quantum Phase Transitions*, 2nd ed. (Cambridge University Press, Cambridge. England, 2011).
[30] M. Ammon and J. Erdmenger, *Gauge/Gravity Duality* (Cambridge University Press, Cambridge, England, 2015).
[31] J. Zaanen, Y.-W. Sun, Y. Liu, and K. Schalm, *Holographic Duality in Condensed Matter Physics* (Cambridge University Press, Cambridge, England, 2015).
[32] G. T. Horowitz and V. E. Hubeny, *Quasinormal Modes of AdS Black Holes and the Approach to Thermal Equilibrium*, Phys. Rev. D **62**, 024027 (2000).
[33] D. T. Son and A. O. Starinets, *Minkowski Space Correlators in AdS/CFT Correspondence: Recipe and Applications*, J. High Energy Phys. 09 (2002) 042.
[34] B. Withers, *Short-Lived Modes from Hydrodynamic Dispersion Relations*, J. High Energy Phys. 06 (2018) 059.
[35] S. Grozdanov, P. K. Kovtun, A. O. Starinets, and P. Tadić, *Convergence of the Gradient Expansion in Hydrodynamics*, Phys. Rev. Lett. **122**, 251601 (2019).
[36] S. Grozdanov, P. K. Kovtun, A. O. Starinets, and P. Tadić, *The Complex Life of Hydrodynamic Modes*, J. High Energy Phys. 11 (2019) 097.
[37] M. P. Heller, A. Serantes, M. Spaliński, V. Svensson, and B. Withers, *Convergence of Hydrodynamic Modes: Insights from Kinetic Theory and Holography*, SciPost Phys. **10**, 123 (2021).
[38] P. Kovtun and L. G. Yaffe, *Hydrodynamic Fluctuations, Long Time Tails, and Supersymmetry*, Phys. Rev. D **68**, 025007 (2003).
[39] M. P. Heller, A. Serantes, M. Spalinski, V. Svensson, and B. Withers, *The Hydrodynamic Gradient Expansion in Linear Response Theory*, arXiv:2007.05524.
[40] M. P. Heller, R. A. Janik, and P. Witaszczyk, *Hydrodynamic Gradient Expansion in Gauge Theory Plasmas*, Phys. Rev. Lett. **110**, 211602 (2013).
[41] N. Abbasi and S. Tahery, *Complexified Quasinormal Modes and the Pole-Skipping in a Holographic System at Finite Chemical Potential*, J. High Energy Phys. 10 (2020) 076.
[42] A. Jansen and C. Pantelidou, *Quasinormal Modes in Charged Fluids at Complex Momentum*, J. High Energy Phys. 10 (2020) 121.
[43] S. Grozdanov, *Bounds on Transport from Univalence and Pole-Skipping*, Phys. Rev. Lett. **126**, 051601 (2021).
[44] C. Choi, M. Mezei, and G. Sárosi, *Pole Skipping Away from Maximal Chaos*, J. High Energy Phys. 02 (2021) 207.
[45] H. Liu, J. McGreevy, and D. Vegh, *Non-Fermi Liquids from Holography*, Phys. Rev. D **83**, 065029 (2011).
[46] M. Cubrovic, J. Zaanen, and K. Schalm, *String Theory, Quantum Phase Transitions and the Emergent Fermi-Liquid*, Science **325**, 439 (2009).
[47] T. Faulkner, H. Liu, J. McGreevy, and D. Vegh, *Emergent Quantum Criticality, Fermi Surfaces, and* AdS_2, Phys. Rev. D **83**, 125002 (2011).
[48] N. Iqbal, H. Liu, and M. Mezei, *Semi-Local Quantum Liquids*, J. High Energy Phys. 04 (2012) 086.
[49] S. Sachdev and J. Ye, *Gapless Spin-Fluid Ground State in a Random Quantum Heisenberg Magnet*, Phys. Rev. Lett. **70**, 3339 (1993).
[50] S. Sachdev, *Holographic Metals and the Fractionalized Fermi Liquid*, Phys. Rev. Lett. **105**, 151602 (2010).
[51] A. Almheiri and J. Polchinski, *Models of* AdS_2 *Backreaction and Holography*, J. High Energy Phys. 11 (2015) 014.
[52] A. Kitaev, *A Simple Model of Quantum Holography, KITP Program: Entanglement in Strongly-Correlated Quantum Matter*, https://online.kitp.ucsb.edu/online/entangled15/.
[53] S. Sachdev, *Bekenstein-Hawking Entropy and Strange Metals*, Phys. Rev. X **5**, 041025 (2015).
[54] J. Maldacena and D. Stanford, *Remarks on the Sachdev-Ye-Kitaev model*, Phys. Rev. D **94**, 106002 (2016).
[55] J. Maldacena, D. Stanford, and Z. Yang, *Conformal Symmetry and Its Breaking in Two Dimensional Nearly Anti-de-Sitter Space*, Prog. Theor. Exp. Phys. **2016**, 12C104 (2016).
[56] K. Jensen, *Chaos in* AdS_2 *Holography*, Phys. Rev. Lett. **117**, 111601 (2016).
[57] J. Engelsöy, T. G. Mertens, and H. Verlinde, *An Investigation of* AdS_2 *Backreaction and Holography*, J. High Energy Phys. 07 (2016) 139.
[58] Y. Gu, X.-L. Qi, and D. Stanford, *Local Criticality, Diffusion and Chaos in Generalized Sachdev-Ye-Kitaev Models*, J. High Energy Phys. 05 (2017) 125.
[59] R. A. Davison, W. Fu, A. Georges, Y. Gu, K. Jensen, and S. Sachdev, *Thermoelectric Transport in Disordered Metals without Quasiparticles: The Sachdev-Ye-Kitaev Models and Holography*, Phys. Rev. B **95**, 155131 (2017).
[60] S. Sachdev, *Universal Low Temperature Theory of Charged Black Holes with* AdS_2 *Horizons*, J. Math. Phys. (N.Y.) **60**, 052303 (2019).
[61] Y. Bardoux, M. M. Caldarelli, and C. Charmousis, *Shaping Black Holes with Free Fields*, J. High Energy Phys. 05 (2012) 054.
[62] T. Andrade and B. Withers, *A Simple Holographic Model of Momentum Relaxation*, J. High Energy Phys. 05 (2014) 101.
[63] J. Zaanen, *Superconductivity: Why the Temperature Is High*, Nature (London) **430**, 512 (2004).
[64] Unlike here, τ_{eq} is often defined by the lifetime of a $k=0$ mode. In our conventions, these examples have $D \to v_{\mathrm{eq}}^2 \tau_{\mathrm{eq}}/2$ in the limit of slow relaxation.
[65] T. Hartman, S. A. Hartnoll, and R. Mahajan, *Upper Bound on Diffusivity*, Phys. Rev. Lett. **119**, 141601 (2017).
[66] A. Lucas, *Constraints on Hydrodynamics from Many-Body Quantum Chaos*, arXiv:1710.01005.
[67] M. Blake, *Universal Charge Diffusion and the Butterfly Effect in Holographic Theories*, Phys. Rev. Lett. **117**, 091601 (2016).
[68] M. Blake, *Universal Diffusion in Incoherent Black Holes*, Phys. Rev. D **94**, 086014 (2016).
[69] M. Blake and A. Donos, *Diffusion and Chaos from near* AdS_2 *Horizons*, J. High Energy Phys. 02 (2017) 013.
[70] M. Blake, R. A. Davison, and S. Sachdev, *Thermal Diffusivity and Chaos in Metals without Quasiparticles*, Phys. Rev. D **96**, 106008 (2017).
[71] H. Guo, Y. Gu, and S. Sachdev, *Transport and Chaos in Lattice Sachdev-Ye-Kitaev Models*, Phys. Rev. B **100**, 045140 (2019).
[72] S. Grozdanov, K. Schalm, and V. Scopelliti, *Black Hole Scrambling from Hydrodynamics*, Phys. Rev. Lett. **120**, 231601 (2018).

[73] M. Blake, H. Lee, and H. Liu, *A Quantum Hydrodynamical Description for Scrambling and Many-Body Chaos*, J. High Energy Phys. 10 (2018) 127.

[74] M. Blake, R. A. Davison, S. Grozdanov, and H. Liu, *Many-Body Chaos and Energy Dynamics in Holography*, J. High Energy Phys. 10 (2018) 035.

[75] M. Blake, R. A. Davison, and D. Vegh, *Horizon Constraints on Holographic Green's Functions*, J. High Energy Phys. 01 (2020) 077.

[76] See Supplemental Material at http://link.aps.org/supplemental/10.1103/PhysRevX.11.031024 for more details on the calculations reported here, which includes Refs. [77–82].

[77] H. Kodama and A. Ishibashi, *Master Equations for Perturbations of Generalized Static Black Holes with Charge in Higher Dimensions*, Prog. Theor. Phys. **111**, 29 (2004).

[78] D. K. Brattan and S. A. Gentle, *Shear Channel Correlators from Hot Charged Black Holes*, J. High Energy Phys. 04 (2011) 082.

[79] X.-H. Ge, K. Jo, and S.-J. Sin, *Hydrodynamics of RN* AdS_4 *Black Hole and Holographic Optics*, J. High Energy Phys. 03 (2011) 104.

[80] R. A. Davison and N. K. Kaplis, *Bosonic Excitations of the* AdS_4 *Reissner-Nordstrom Black Hole*, J. High Energy Phys. 12 (2011) 037.

[81] R. A. Davison and A. Parnachev, *Hydrodynamics of Cold Holographic Matter*, J. High Energy Phys. 06 (2013) 100.

[82] M. Kaminski, K. Landsteiner, J. Mas, J. P. Shock, and J. Tarrio, *Holographic Operator Mixing and Quasinormal Modes on the Brane*, J. High Energy Phys. 02 (2010) 021.

[83] S. A. Hartnoll and D. M. Hofman, *Locally Critical Resistivities from Umklapp Scattering*, Phys. Rev. Lett. **108**, 241601 (2012).

[84] M. Edalati, J. I. Jottar, and R. G. Leigh, *Shear Modes, Criticality and Extremal Black Holes*, J. High Energy Phys. 04 (2010) 075.

[85] U. Moitra, S. K. Sake, and S. P. Trivedi, *Near-Extremal Fluid Mechanics*, J. High Energy Phys. 02 (2021) 021.

[86] M. Edalati, J. I. Jottar, and R. G. Leigh, *Transport Coefficients at Zero Temperature from Extremal Black Holes*, J. High Energy Phys. 01 (2010) 018.

[87] M. Edalati, J. I. Jottar, and R. G. Leigh, *Holography and the Sound of Criticality*, J. High Energy Phys. 10 (2010) 058.

[88] Another family of holographic $z = 1$ fixed points was studied in Refs. [89,90]. These geometries do not have a slow mode, but in a certain limit also display an emergent SL(2,R) symmetry and a spectrum of infrared mode similar to the one studied in this work.

[89] P. Betzios, U. Gürsoy, M. Järvinen, and G. Policastro, *Quasinormal Modes of a Strongly Coupled Nonconformal Plasma and Approach to Criticality*, Phys. Rev. D **97**, 081901(R) (2018).

[90] P. Betzios, U. Gürsoy, M. Järvinen, and G. Policastro, *Fluctuations in a Nonconformal Holographic Plasma at Criticality*, Phys. Rev. D **101**, 086026 (2020).

[91] T. Faulkner and J. Polchinski, *Semi-Holographic Fermi Liquids*, J. High Energy Phys. 06 (2011) 012.

[92] D. Nickel and D. T. Son, *Deconstructing Holographic Liquids*, New J. Phys. **13**, 075010 (2011).

[93] J. de Boer, M. P. Heller, and N. Pinzani-Fokeeva, *Effective Actions for Relativistic Fluids from Holography*, J. High Energy Phys. 08 (2015) 086.

[94] J. de Boer, M. P. Heller, and N. Pinzani-Fokeeva, *Holographic Schwinger-Keldysh Effective Field Theories*, J. High Energy Phys. 05 (2019) 188.

[95] P. Glorioso, M. Crossley, and H. Liu, *A Prescription for Holographic Schwinger-Keldysh Contour in Non-Equilibrium Systems*, arXiv:1812.08785.

[96] D. T. Son, *Toward an AdS/Cold Atoms Correspondence: A Geometric Realization of the Schrödinger Symmetry*, Phys. Rev. D **78**, 046003 (2008).

[97] P. T. Brown, D. Mitra, E. Guardado-Sanchez, R. Nourafkan, A. Reymbaut, C.-D. Hébert, S. Bergeron, A.-M. S. Tremblay, J. Kokalj, D. A. Huse *et al.*, *Bad Metallic Transport in a Cold Atom Fermi-Hubbard System*, Science **363**, 379 (2019).

[98] J. C. Zhang, E. M. Levenson-Falk, B. J. Ramshaw, D. A. Bonn, R. Liang, W. N. Hardy, S. A. Hartnoll, and A. Kapitulnik, *Anomalous Thermal Diffusivity in Underdoped* $\mathrm{YBa_2Cu_3O_{6+x}}$, Proc. Natl. Acad. Sci. U.S.A. **114**, 5378 (2017).

[99] J. Zhang, E. D. Kountz, E. M. Levenson-Falk, D. Song, R. L. Greene, and A. Kapitulnik, *Thermal Diffusivity Above the Mott-Ioffe-Regel Limit*, Phys. Rev. B **100**, 241114 (2019).